Biosensors and Bioelectronics 25 (2009) 378–382

Contents lists available at ScienceDirect

Biosensors and Bioelectronics

journal homepage: www.elsevier.com/locate/bios

An electrochemical biosensor for ultratrace terbium based on Tb^{3+} promoted conformational change of human telomeric G-quadruplex

Jing Zhang[a,b], JingHua Chen[a,c], RongChun Chen[a], GuoNan Chen[a], FengFu Fu[a,*]

[a] Ministry of Education Key Laboratory of Analysis and Detection for Food Safety, and Department of Chemistry, Fuzhou University, Fuzhou, Fujian, 350108, China
[b] Pharmaceutical Department of Fujian College of Medical Occupation and Technology, Fuzhou 350101, China
[c] Department of Pharmaceutical Analysis, Faculty of Pharmacy, Fujian Medical University, Fuzhou 350004, China

ARTICLE INFO

Article history:
Received 17 June 2009
Received in revised form 23 July 2009
Accepted 23 July 2009
Available online 3 August 2009

Keywords:
Electrochemical biosensor
Reversible switch
Terbium
G-quadruplex
Human telomeric

ABSTRACT

A new electrochemical biosensor for the monitoring of ultratrace terbium based on the conformational change of DNA containing a single guanine (G)-rich stretch was described here. The biosensor was fabricated by immobilizing a thiolated DNA containing a single G-rich stretch on the gold surface as probe surface. The G-rich DNA probe was found to be capable of changing its configuration from flexible single-stranded structures to rigid tetramolecular G-quadruplex in the presence of terbium III, which provided a switchable charge transport path for the oxidation of $[Fe(CN)_6]^{4-}$. The switchable surface provided a sensing platform for the single-step and reagentless detection of Tb^{3+}. Using this reusable electrochemical sensing platform, a simple, rapid, and selective biosensor for the determination of ultratrace terbium ions with a detection limit of 6.0×10^{-11} M has been developed. The success in the present biosensor served as a significant step toward the development of monitoring ultratrace Tb^{3+} in river water or seawater.

1. Introduction

The control of switchable surface that performs useful functions is of central importance to biosensor (Chen and Mao, 2004), and the unique molecular recognition properties of DNA make it an extremely versatile material for design of novel modified layer and has been extensively studied in nucleic acid nanodevices (Li et al., 2008) Recently, Guanine-rich (G-rich) oligonucleotides were reported to be capable of forming in vitro four-stranded structures, based on the guanine quartet, known as G-quadruplexes, G4 DNA or tetraplex DNA (Guschlbauer et al., 1990). Interest in G-quadruplex structural motifs is stimulated since several biological important guanine-rich genomic regions were discovered including telomeres, immunoglobulin switch region, some oncogene promoters and others (Simonsson, 2001). In general, the formation of guanine quadruplexes requires the presence of certain metal cations, mainly alkali ions such as K^+ and Na^+, etc. These cations are positioned within the helical core of quadruplex between adjacent guanine quartets, coordinated by eight O-6 oxygen atoms (Galezowska et al., 2007). Based on the conformational change of DNA sequence caused by above alkali ions, Wu et al. (2008) developed an on/off electronic nanoswitch for the determination of K^+, and Zhang et al. (2008) also demonstrated a switchable solid/liquid surface for the charge transport of $[Fe(CN)_6]^{4-}$ using G-rich DNA probes as modified layer and K^+ as stimuli. Their results demonstrated that the conformational change of G-quardruplex DNA could also be used as "smart surface". In contrast to alkali cations, the formation of G-quadruplexes promoted with trivalent cations such as lanthanide ions has seldom been reported. Nagesh et al. (1992) first reported on the interactions between trivalent cation, Tb^{3+}, and telomeric oligonucleotide containing tetrahymena sequence, $d(T_2G_4)_4$, and monitored the quadruplex stability based on the luminescence properties of Tb^{3+} and the energy transfer from DNA bases. They found that the formation of G-quadruplex structure of $d(T_2G_4)_4$ is highly dependent on the presence of Tb^{3+}. Stimulated by their study, we herein report a novel electrochemical biosensor for the monitoring of ultratrace Tb^{3+} via G-quadruplex probe, which bearing human telomeric repeat sequence d(G3T2AG3T2AG3-T2AG3), (htel21).

As one of important member of rare earth elements (REEs), terbium is widely used in cathode-ray tubes, magnets optical computer memories, bioanalytical field and so on (Gupta et al., 2008; Belousoff et al., 2009). Terbium together with other REEs has also been wildly used as tracer in geochemical field (Kay and Gast, 1973; Taylor and McLennan, 1988). Dissolved Tb and other REEs in river or ocean were expected to reflect the global or local ocean circulation, biogeochemical cycling and redox condition (Kagi et al., 2004; Wyndham et al., 2004). Therefore, the determination of Tb is of great significance because of the increasing interest in geochemistry and bioinorganic chemistry. So far, the most techniques for

* Corresponding author. Tel.: +86 591 28306608; fax: +86 591 28306608.
E-mail address: fengfu@fzu.edu.cn (F. Fu).

0956-5663/$ – see front matter © 2009 Elsevier B.V. All rights reserved.
doi:10.1016/j.bios.2009.07.029

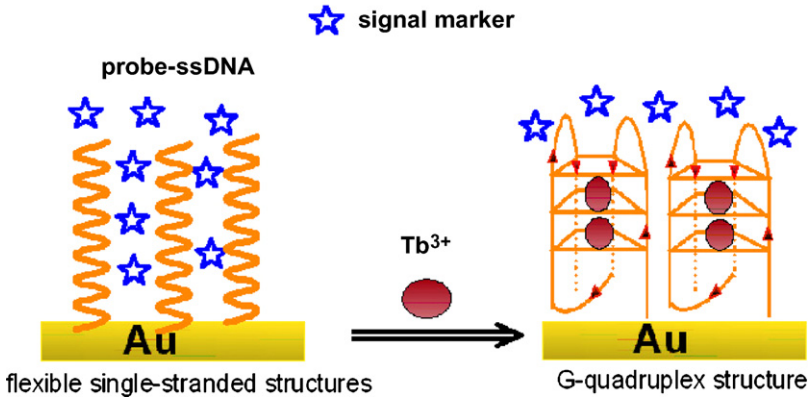

Fig. 1. Diagram of the experimental principle of the electrochemical biosensor.

the determination of ultratrace terbium are isotope dilution mass spectrometry (ID-MS) (Goldstein and Jacobsen, 1988; Tanaka et al., 1990) and inductively coupled plasma mass spectrometry (ICP-MS) (Vicente et al., 1998). However, these methods require sophisticated apparatus, have a high assay cost and cannot be used to monitor Tb in situ. Due to the aforementioned limitations of ID-MS and ICP-MS, it is essential to develop a sensor for the monitoring of ultratrace terbium. The success in the present biosensor provided the possibility of monitoring ultratrace Tb^{3+} in river water or seawater.

2. Experimental

2.1. Reagents

The G-rich oligonucleotide designed was synthesized by TaKaRa biotechnology Co., Ltd. (Dalian, China), and its base sequence is: -5′-SH-$(CH_2)_6$-TTT TTT TTT TTT TTT TTT TTg ggt tag ggt tag ggt tag gg-3′. A foreign DNA of -5′-ccc taa ccc taa ccc taa ccc-3′ was used to test the selectivity of designed G-rich oligonucleotide. All oligonucleotides stock solutions (100 μM) were prepared in TE solution (10 mM Tris–HCl, 1.0 mM EDTA, pH 8.00) and kept frozen. More dilute solution was also prepared in the same TE solution. Tris-(hydroxymethyl) aminomethane, ethylenediaminetetraacetic acid (EDTA), mercaptohexanol (MCH) and potassium ferrocyanide ($K_4Fe(CN)_6$) were purchased from Sigma–Aldrich company (USA), and tris(2-carboxyethyl) phosphine hydrochloride (TCEP) was purchased from Shanghai Sangon Biological Engineering Technology Services Reagents Co., Ltd. (China). Tb^{3+} solution was prepared by dissolving $Tb(NO_3)_3$ (Wako Pure Chemical Industries Co., Ltd., Japan) in 2% nitric acid solution. All chemicals were of analytical grade, and sterilized Milli-Q water was used in all experiment. River water was collected in Minjiang River (Fujian, China) and was immediately filtrated with a 0.45 μm Nuclepore filter before the analysis of Tb^{3+}.

2.2. Electrochemical measurements

A CHI 660C Electrochemical Workstation (CH Instrument, USA) was used for the cyclic voltammograms (CVs) and electrochemical impedance spectra (EIS) measurements at room temperature. The electrochemical system consisted of a working electrode (a gold disk electrode modified with DNA probe), a platinum wire auxiliary electrode and a Ag/AgCl reference electrode. CVs at different stages of the biosensor preparation were measured in 10 mM Tris–HCl solutions (pH 7.0) containing 10 mM $Fe(CN)_6]^{3-/4-}$ at a scan rate of 100 mV/s in a potential range between −0.2 and +0.8 V, and EIS was measured in TE solution (10 mM Tris–HCl, 1.0 mM EDTA, pH 8.00) containing 10 mM $[Fe(CN)_6]^{3-/4-}$ in the frequency range between 100 kHz and 1.0 Hz.

2.3. Fabrication of the electrochemical biosensor

A gold disk electrode (2 mm diameter) was first polished to obtain mirror surface with 0.05 μm alumina powder, followed by sonication in ethanol and water for 5 min respectively. Then the electrode was electrochemically treated in 0.5 M H_2SO_4 by cycling the potential between −0.4 and +1.5 V until the CVs characteristic of a cleaning surface was observed. After drying the electrode with nitrogen gas, the gold electrode (GE) was incubated in 1 μM thiolated G-rich oligonucleotide solution at room temperature for 1 h to construct the electrochemical biosensor. Subsequently, the G-rich oligonucleotide modified GE was further treated with 1 mM MCH for 2 h in order to obtain well-aligned DNA monolayers.

2.4. Electrochemical detection of Tb^{3+}

The electrochemical biosensor (GE modified with G-rich DNA probe) was directly incubated in a sample containing Tb^{3+} at room temperature for 3 min. Then, take out the biosensor and put it into 5.0 mL TE solution (pH 8.00) containing 10 mM $[Fe(CN)_6]^{3-/4-}$, and the EIS were measured with above method. The baseline-subtracted *R*et (resistance of electron transfer) was used to calculate the concentration of Tb^{3+}.

3. Results and discussion

3.1. Experimental principle

The experimental principle of the electrochemical biosensor was illustrated in Fig. 1. As shown in Fig. 1, in the absence of Tb^{3+}, G-rich DNA probes immobilized on the surface of GE have flexible single-stranded structures. Therefore, $[Fe(CN)_6]^{4-}$ in solution can easily penetrate through the DNA monolayer, reach the surface of GE, and is then oxidized to form $[Fe(CN)_6]^{3-}$. However, in the presence of Tb^{3+}, the G-rich DNA probes changed conformation to form compact quadruplexs. Because ssDNA and G-quadruplex DNA possess the same amount of charged groups, the formation of G-quadruplex enhances the surface charge density and accordingly repels the negatively charged $[Fe(CN)_6]^{4-}$ (Simonsson, 2001; Radi and O'Sullivan, 2006). Hence, the penetration of $[Fe(CN)_6]^{4-}$ through the DNA monolayer is hindered, which in turn leads to decreased electrochemical response. This reversible process can be easily monitored electrochemically and can be used as reagentless, reusable electrochemical sensing platform for Tb^{3+} detection.

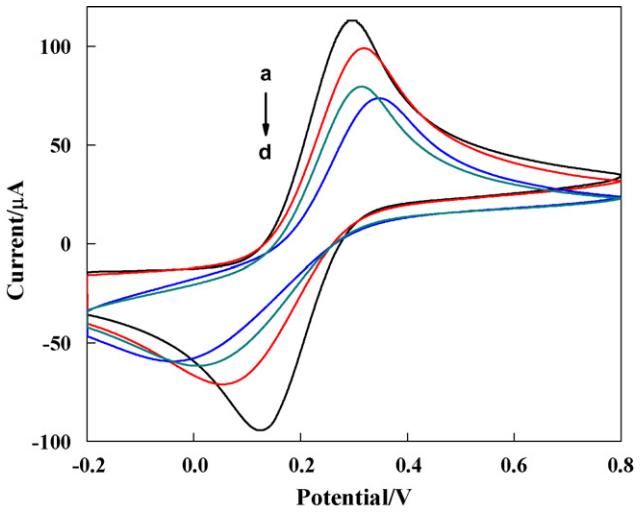

Fig. 2. CVs of 10 mM $Fe(CN)_6]^{3-/4-}$ at different stages of the electrochemical biosensor preparation. (a) bare GE; (b) G-rich DNA probe modified GE; (c) G-rich DNA probe/MCH modified GE; (d) G-rich DNA probe/MCH/Tb^{3+} modified GE. Data obtained in 10 mM Tris–HCl solutions (pH 7.0) containing 10 mM $Fe(CN)_6]^{3-/4-}$ at a scan rate of 100 mV/s.

3.2. Electrochemical studies at different stages of the electrochemical biosensor preparation

The proposed mechanism was tested by cyclic voltammetry of a fairly reversible redox couple $[Fe(CN)_6]^{3-/4-}$ at different stages of the electrochemical biosensor preparation. The CVs of 10 mM $[Fe(CN)_6]^{3-/4-}$ on different surface were shown in Fig. 2. From CVs shown in Fig. 2, it was clearly observed that the reversible redox peaks of $[Fe(CN)_6]^{4-}$ have a highest peak current on the bare GE surface (line a), and self-assembly of the thiolated G-rich DNA probe monolayer on the surface of GE induces the decrease of the reversible peaks significantly (line b). Above results clearly indicated that the electrostatic repulsion between anionic $[Fe(CN)_6]^{3-/4-}$ and the negatively charged DNA backbones considerably hindered the electron transfer from redox molecules to the electrode surface. When exposing the G-rich DNA probe modified GE to MCH solution, the insulating property further increases (line c) since the uncovered gold surface was blocked and the net negative dipole of the alcohol terminus can repel the negatively charged electroactive molecules (Wu et al., 2008). After treating the G-rich DNA probe/MCH modified GE with 2.05×10^{-9} mol L^{-1} Tb^{3+} solution, a further decrease on the redox peaks was observed (line d). The reason was that the compact G-quadruplex structure "switches off" the charge transport path of $[Fe(CN)_6]^{3-/4-}$. The increase of overvoltage and the decrease of current in curve d, meant that $[Fe(CN)_6]^{3-/4-}$ need higher energy to penetrate through the G-quadruplex DNA monolyer and therefore less $[Fe(CN)_6]^{3-/4-}$ could be oxidized on the surface of electrode (Wu et al., 2008).

In a further control experiment, the treatment of foreign DNA with Tb^{3+} did not bring significant changes on the redox response of $[Fe(CN)_6]^{3-/4-}$, indicating that this switchable conformational

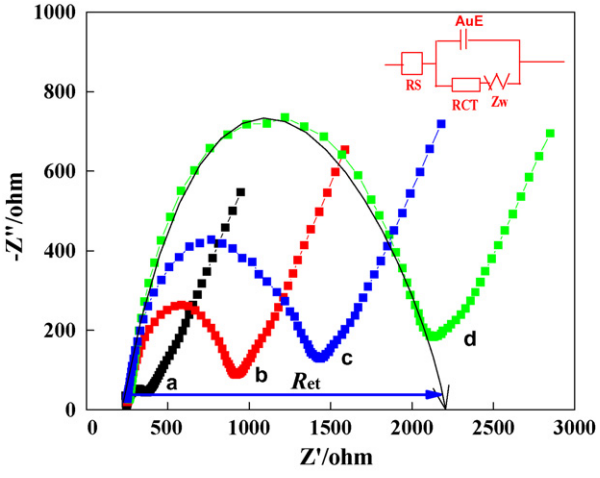

Fig. 3. Nyquist plots of EIS obtained in TE solution (10 mM Tris–HCl, 1.0 mM EDTA, pH 8.00) containing 10 mM $[Fe(CN)_6]^{3-/4-}$. (a) Bare GE; (b) G-rich DNA probe modified GE; (c) G-rich DNA probe/MCH modified GE; (d) G-rich DNA probe/MCH/Tb^{3+} modified GE. The biased potential was 0.20 V (versus Ag/AgCl). The frequency was from 100 kHz to 1.0 Hz and the amplitude was 5.0 mV. The inset shows the equivalent circuit applied to fit the impedance spectroscopy. EIS was presented as Nyquist plot (Z', real impedance, versus Z'', imaginary impedance) using CH Instruments software. The semicircle on the Nyquist plot, which diameter corresponds to the real impedance on Z' axis, was used to calculate *R*et value.

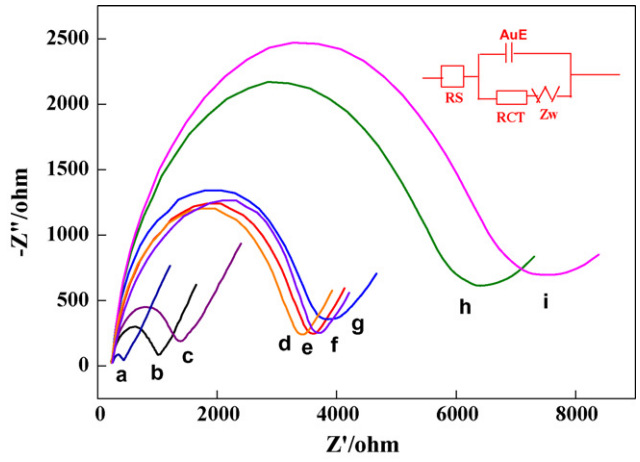

Fig. 4. Nyquist plots of EIS obtained in TE solution (10 mM Tris–HCl, 1.0 mM EDTA, pH 8.00) containing 10 mM $[Fe(CN)_6]^{3-/4-}$ at G-rich DNA probe modified GE (b), G-rich DNA probe/MCH/Tb^{3+}(5.46×10^{-7} M) modified GE (e), and G-rich DNA probe/MCH/Tb^{3+}(5.46×10^{-7} M) modified GE in the presence of 4 M Na^+ (a), 3 M Na^+ (c), 0.05 M Dy^{3+} (d), 0.05 M Gd^{3+} (f), 0.05 M Na^+ (g), 0.31 M Na^+ (h), 0.46 M Na^+ (i). Other conditions are the same as those in Fig. 3.

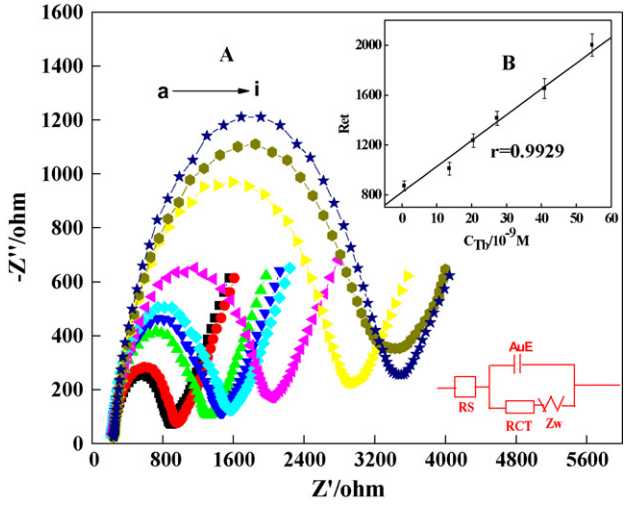

Fig. 5. (A) EIS of the electrochemical biosensor designed in this study in different concentrations of Tb^{3+}. Tb^{3+} concentration is: (a) 0 M; (b) 6.83×10^{-10} M; (c) 13.6×10^{-10} M; (d) 20.5×10^{-10} M; (e) 27.3×10^{-10} M; (f) 40.9×10^{-10} M; (g) 54.6×10^{-10} M; (h) 68.3×10^{-10} M; (i) 70.2×10^{-10} M. Other experimental conditions are the same as that in Fig. 3. (B) The plot of *R*et versus Tb^{3+} concentration. Error bars = ±relative standard deviation. Other conditions are the same as those in Fig. 3.

Table 1
Determination of Tb^{3+} in artificial river water samples ($n = 5$).

Tb^{3+} added (nM)	Concentration detected with this method (nM)	Recovery (%)	RSD (%)	Concentration detected by ICP-MS (nM)
1.0	1.04	104	5.2	0.99
2.0	1.97	98.5	4.4	2.02
3.0	2.98	99.3	3.9	2.96

change is specific for the G-rich sequence. All above results verified that Tb^{3+} promoted the conformational transition of the G-rich DNA from flexible single-stranded structures to G-quadruplex. In the presence of Tb^{3+}, the compact G-quadruplex structure "switches off" the charge transport path of $[Fe(CN)_6]^{3-/4-}$; while in the absence of Tb^{3+}, this path is "switched on". The "switched on/off" characteristic forms the basis of electrochemical quantification of Tb^{3+}.

3.3. Electrochemical impedance spectra studies at different stages of the electrochemical biosensor preparation

The performance of the electrochemical biosensor was further evaluated by EIS. Fig. 3 showed the nyquist plots of impedance spectra at different stages of the electrochemical biosensor preparation. The bare GE exhibited the smallest semicircle at high frequency region (curve a). When the GE was modified with thiolated G-rich DNA probe, the *R*et increased to 270 Ω (curve b). This should be attributed to fact that self-assembled DNA monolayer, which has a single strand nucleic acid with negative charges on its phosphate backbone, makes an electrostatic repulsive force to $[Fe(CN)_6]^{3-/4-}$. After the MCH in which a short-chain alkyl molecule was employed to occupy the left bare sites on GE was added, the *R*et further increased to 429 Ω (curve c). Then, the G-rich DNA probe/MCH modified GE was further treated with 2.05×10^{-9} M Tb^{3+} solution, the *R*et greatly increased to 739 Ω (curve d). This fact strongly suggested that the compact G-quadruplex structure is generated and the transfer of redox couple $[Fe(CN)_6]^{3-/4-}$ to the surface of GE is prohibited in the presence of Tb^{3+}. The results of EIS also indicated that our biosensor indeed works as we expected. It was also found that the change of the *R*et in EIS was much more sensitive than the change of peak currents in cyclic voltammograms (the detection limit of Tb^{3+} based on the change of peak currents was calculated to be 2.9×10^{-9} M, whereas, that based on the change of *R*et was calculated to be 6.0×10^{-11} M). Therefore, EIS detection model is utilized in this work to obtain a higher sensitivity.

3.4. The interference of other metallic cations

Some metallic cations are known to stabilize G-quadruplex formation, these ions can compete with terbium ion to enter the quadruplex cavity (Guschlbauer et al., 1990; Simonsson, 2001). Fig. 4 showed the *R*et trace of htel21 titrated with Tb^{3+} ion in the absence and the presence of different concentrations of NaCl. Our results showed that when the concentration of NaCl is smaller than 0.05 M, only a few increase in *R*et was observed (see curves e and g). However, when the concentration of NaCl is bigger than 0.05 M, there is a great increase in *R*et with the increase of Na^+, reflecting the equilibrium competition between Tb^{3+} and Na^+ ions for the binding sites on G-quadruplex. Our experimental results indicated that 100,000-fold of sodium ion does not affect the detection of Tb^{3+}. It was found that an extremely higher NaCl concentration (>3 M) led to a tremendous decrease in *R*et (see curves a and c), we proposed an explanation that too many Na^+ ions caused the collapse of G-quadruplex structure. We further investigated other metallic ions, including monovalent cations such as K^+, Li^+ and divalent cations such as Mg^{2+}. The ability of these cations to compete with Tb^{3+} ion decreased in the order of $Mg^{2+} > K^+ > Li^+$, and our results indicated that 120,000-fold of Mg^{2+} ion does not affect the detection of Tb^{3+}.

It was well known, all lanthanides showed similar chemical characteristics, and it is possible that the existence of other lanthanide's ions will affect the detection of Tb^{3+}. In order to further investigate if other members of rare earth element will disturb the detection of Tb^{3+}, Dy^{3+} and Gd^{3+} were selected as the representatives of other lanthanides and were used to test the selectivity of our sensor since their chemical characteristic is the most similar to that of Tb^{3+}. The results (see curves d, f and e in Fig. 4) showed that 100,000-fold of Dy^{3+} (0.05 M) and Gd^{3+} (0.05 M) ions do not affect the detection of Tb^{3+}, indicating the good selectivity of our sensor. As we mentioned above, Dy^{3+} and Gd^{3+} are the most similar to Tb^{3+} in chemical characteristic among all lanthanide's ions. In addition, the concentration ratios of other lanthanide's ions to Tb^{3+} are much lower than 100,000 in nature. Therefore, the fact that the influence of 0.05 M Dy^{3+} and Gd^{3+} on the detection of Tb^{3+} has not been observed indicated that other lanthanide's ions will not affect the detection. For above reason, the influence of other lanthanide's ions on the detection of Tb^{3+} has not been further investigated in this study.

3.5. The sensitivity of the electrochemical biosensor

The quantitative behavior of the electrochemical biosensor fabricated with htel21 probes was assessed. The EIS of the electrochemical biosensor in the presence of different concentrations of Tb^{3+} are shown in Fig. 5. The *R*et showed a fine linear relationship with the concentration of Tb^{3+} in the range from 0.683×10^{-9} to 5.46×10^{-9} M (see Fig. 5B). The regression equation was *R*et (Ω) = 799.59 + 21.514 × C_{Tb} (10^{-9} M) and the regression coefficient (r) was 0.9929. The detection limit for Tb^{3+} was calculated to be 6.0×10^{-11} M and RSD ($n = 5$) was calculated to be 4.5% for 2.05×10^{-9} M Tb^{3+}, indicating that the electrochemical biosensor developed in this study has a high sensitivity and a good reproducibility.

3.6. Analysis of Tb^{3+} in artificial river water

Three artificial river water samples were composed by adding different concentration of Tb^{3+} in real river water collected in Minjiang river (Fujian, China), and the concentrations of Tb^{3+} in them were determined with the electrochemical biosensor. The results are shown in Table 1 together with the data determined with inductively coupled plasma mass spectrometry (ICP-MS, Agilent 750ce, USA). The results obtained with our biosensor are consistent with those obtained with ICP-MS and have a RSD < 5.2% ($n = 5$), indicating that the new electrochemical biosensor has a good selectivity, accuracy and reproducibility.

4. Conclusions

We developed here a novel electrochemical biosensor by immobilizing a thiolated DNA containing a single G-rich stretch on the gold surface as probe surface. Tb^{3+} can promote the conformational change of the G-rich probe, this provides an "on-off" path for the transport of $[Fe(CN)_6]^{3-/4-}$. We characterized the electrochemical properties of the switchable surface and demonstrated that it can be

used as sensing platform for the single-step and reagentless detection of Tb^{3+}. The electrochemical biosensor developed in this study might be repeatedly regenerated under exceptionally gentle conditions due to the highly reversible conformational change, and has a much lower detection limit of 6.0×10^{-11} M for Tb^{3+}. The success in the present electrochemical biosensor served as a significant step toward the development of monitoring ultratrace Tb^{3+} in river water or seawater.

Acknowledgements

This work was financially support by the National Natural Science Foundation of China (40875087, 20735002) and Education Department of Fujian Province (XSJRC2007-03) and National Science Foundation of Fujian Province (2009J01023).

References

Belousoff, M.J., Ung, P., Forsyth, C.M., Tor, Y., Spiccia, L., Graham, B., 2009. J. Am. Chem. Soc. 131, 1106–1114.
Chen, Y., Mao, C., 2004. J. Am. Chem. Soc. 126, 8626–8627.
Galezowska, E., Gluszynska, A., Juskowiak, B., 2007. J. Inorg. Biochem. 101, 678–685.
Goldstein, S., Jacobsen, S., 1988. Earth Planet. Sci. Lett. 89, 35–47.
Gupta, V.K., Singh, A.K., Gupta, B., 2008. Anal. Bioanal. Chem. 390, 2171–2181.
Guschlbauer, W., Chantot, J.F., Thiele, D.J., 1990. Biomol. Struct. Dyn. 8, 491–511.
Kagi, T.A., Hashimoto, Y., Fu, F.-F., Tsuno, H., Tao, H., Nakano, Y., 2004. Geochim. Cosmochim. Acta 68, 2265–2273.
Kay, R.W., Gast, P.W., 1973. J. Geol. 81, 653–682.
Li, D., Wieckowska, A., Willner, I., 2008. Angew. Chem. Int. Ed. 47, 3297–3931.
Nagesh, N., Bhargava, P., Chatterji, D., 1992. Biopolymers 32, 1421–1424.
Radi, A.E., O'Sullivan, C.K., 2006. Chem. Commun. 32, 3432–3434.
Simonsson, T., 2001. Biol. Chem. 382, 621–628.
Tanaka, M., Shimizu, H., Masuda, A., 1990. Geochem. J. 24, 39–46.
Taylor, S.R., McLennan, S.M., 1988. Handbook on the Physics and Chemistry of Rare Earth. vol. 11. Elsevier, New York, pp. 435–479.
Vicente, O., Padro, A., Martinez, L., Olsina, R., Marchevsky, E., 1998. Spectrochim. Acta B 53, 1281–1287.
Wu, Z.S., Chen, C.R., Shen, G.L., Yu, R.Q., 2008. Biomaterials 29, 2689–2696.
Wyndham, T., McCulloch, M., Fallon, S., Alibert, C., 2004. Geochim. Cosmochim. Acta 68, 2067–2080.
Zhang, J., Wan, Y., Wang, L.H., Song, S.P., Li, D., Fan, C.H., 2008. Electrochem. Commun. 10, 1258–1260.